Carbohydrate Polymers 101 (2014) 1101–1108

Contents lists available at ScienceDirect

Carbohydrate Polymers

journal homepage: www.elsevier.com/locate/carbpol

Mannose-conjugated chitosan nanoparticles loaded with rifampicin for the treatment of visceral leishmaniasis

Pramila Chaubey*, Brahmeshwar Mishra

Department of Pharmaceutics, Indian Institute of Technology (Banaras Hindu University), Varanasi 221005, India

ARTICLE INFO

Article history:
Received 11 July 2013
Received in revised form 10 October 2013
Accepted 11 October 2013
Available online 23 October 2013

Keywords:
Mannose-conjugated chitosan
Nanoparticles
Macrophages
Rifampicin
Leishmaniasis

ABSTRACT

The aim of current research work was to develop and investigate the potential of rifampicin (RIF) loaded mannose-conjugated chitosan nanoparticulate system for selective delivery to the macrophages in the management of visceral leishmaniasis (VL). RIF loaded mannose-conjugated chitosan nanoparticles (mCNPs) were prepared and characterized for shape, size, entrapment efficiency and in vitro drug release. The in vivo bio-distribution in albino rats and ex vivo drug uptake by macrophage were also evaluated. It was observed that extent of accumulation of mCNPs in macrophage rich organs, particularly in liver and spleen, were significantly higher compared to free drug. Ex vivo uptake of mCNPs was 2.31 times higher compared to unconjugated chitosan nanoparticles (CNPs). The macrophage uptake of mCNPs was inhibited significantly on pre-incubation with 0.05 M mannose in a parallel experiment, being suggestive of receptor mediated uptake of mannosylated nanoparticles. Our results indicate that mCNPs could be a promising carrier for selective delivery of RIF to macrophages for effective management of VL.

1. Introduction

Intracellular parasites, such as *P. malariae*, *Mycobacterium tuberculosis*, *Leishmania species* and so on, are taken up by macrophages via phagocytosis, and are resistant to the bio-defence mechanisms of macrophages and survive/multiply intracellularly in these cells. Thus, severe visceral infections are frequently induced by these intracellular parasites (Ferrari, Langen, Naito, & Pieters, 1999). Visceral Leishmaniasis (VL), a disease caused by obligate intracellular protozoan parasites (single celled microorganisms) of genus *Leishmania*, is considered as the second largest parasitic cause of death after malaria. Neglected by researchers and funding agencies, an estimated numbers of new VL cases are 500,000 per annum, with approximately 50,000 deaths each year. Its incidence is increasing, particularly in association with the AIDS pandemic (Marty & Rosenthal, 2002; Murray, 2004). One of the issues in developing drugs against leishmaniasis is delivery of compounds to the parasite which is found within a phago-lysosomal vacuole (PV) within macrophages (Chellat, Merhi, Moreau, & Yahia, 2005). A possible solution is to use receptor specific ligand-polymer conjugates to deliver compounds to the parasite (Duncan, 2003). Macrophages possess various surface receptors such as fucose receptors, mannose, galactose, and many others. These receptors involve the sugar recognition mechanism whereby receptors can recognize the corresponding sugars on the non-reducing terminal of sugar chains and mediate cellular uptake (Wadhwa & Rice, 2003). Subsequent internalization of the carrier system leads to accumulation of the drug in the target cells and exclusion from non target cells (Jain et al., 2008). Therefore, the success of the selective delivery to macrophages crucially depends on the ability to develop ligand decked carrier systems for the desired pharmacological action. Inadequate specificity for macrophages and poor internalization of drug-carrier systems are critical obstacles to their success (Yeeprae, Kawakami, Yamashita, & Hashida, 2006).

Polymeric nanoparticles are colloidal carriers having attractive physicochemical properties such as size, surface potential, and hydrophilic-hydrophobic balance (Sakuma & Ohshima, 1990). Although various biodegradable polymers of natural origin such as cellulose, starch and gelatin are largely in use as drug carriers in targeted drug delivery system, chitosan considered to be a good candidate because it is biocompatible, biodegradable and its chemical structure allows specific modifications without too many difficulties at the C-2 position (Rinaudo, 2006). Immunostimulating activity of chitosan, such as increasing the accumulation and activation of macrophages and natural killer cells, inducing cytokines, and cytotoxic T cell response, has also been reported for several years (Busilacchi, Gigante, Mattioli-Belmonte, Manzotti, & Muzzarelli, 2013; Muzzarelli, 2010; Seferian & Martinez, 2001).

Rifampicin (RIF) is primarily an antitubercular drug, but has also been reported to have anti-leishmanial activity (Neuber, 2008). It preferentially accumulates in cells, distributes in the cytosol of

* Corresponding author. Tel.: +91 0542 6702748;
fax: +91 0542 2368428/2368160; mobile: +91 8860412500.
E-mail address: cpramil@gmail.com (P. Chaubey).

0144-8617/$ – see front matter © 2013 Elsevier Ltd. All rights reserved.
http://dx.doi.org/10.1016/j.carbpol.2013.10.044

the cell and shows very good solubility at phago-lysosomal pH (Bakker-Woudenberg, 1995). One of the routes of phagocytosis of *leishmania* parasite is dependent on the interaction between the mannose-containing lipopolysaccharides on the parasite cell surface and the macrophage mannose receptors. Therefore, by mimicking the same invasion process the mannose-conjugated carriers can effectively be taken up by the cells containing the intracellular pathogens, and hence could increase the ability of drug to reach its target, and to act in the corresponding environment. In the present study, mannose-conjugated chitosan nanoparticles (mCNPs) based on mannose-conjugated biodegradable chitosan polymer (M-chitosan) was designed and synthesized for the purpose of improving macrophage specificity, enhancing cellular uptake, and reducing toxicity. The formulation could also be promising in the treatment of leishmaniasis associated with tuberculosis.

2. Materials and methods

2.1. Material

Chitosan (from shrimp shell, molecular weight 150 kDa; deacetylation degree 85%) and RIF were received as a gift samples from Central Institute of Fisheries Technology, Cochin, Kerala and Lupin Pharmaceuticals, Inc., Pune, respectively. Mannose was purchased from SD Fine Chemicals, Mumbai. Trichloro acetic acid (TCA), ammonium acetate, RPMI 1640 and Fluorescein 5 (6)-isothiocyanate (FITC) were purchased from Hi Media, Mumbai. Sodium triacetoxyborohydride [$NaBH(OAc)_3$] was purchased from Sigma-Aldrich. Sodium tripolyphosphate (TPP) and 12 well culture plates were purchased from Himedia, Mumbai, India. Acetonitrile (ACN) was purchased from Merck Ltd., Mumbai. Other organic chemical and solvents used were of reagent grade and used as directed.

2.2. Animals

Healthy male albino rats (Charles Foster strain; mean weight – 220 g) were obtained from Central Animal House, Banaras Hindu University. The animals were maintained in accordance with the Committee for the Purpose of Control and Supervision of Experiments on Animals, Delhi, India. All animal studies were carried out in accordance with protocols approved by the Central Animal Ethics Committee (CAEC) at the Institute of Medical Sciences, Banaras Hindu University (CAEC approval number Dean/10-11/542). The animals were provided with food and water ad libitum. All efforts were made in order to reduce animal suffering.

2.3. Synthesis of M-chitosan

M-chitosan was synthesized as described by Yalpani and Laurance (1984) with little modification. Mannose conjugation was carried out by reductive amination of chitosan with D-mannose in the presence of sodium triacetoxyborohydride [$NaBH(OAc)_3$] (reductive amination reagent). In brief, chitosan was dissolved with stirring in 1% aqueous acetic acid of pH 5.5. An aqueous solution of D-mannose and sodium triacetoxyborohydride was prepared. This solution was then, added to the resulting viscous solution of chitosan while stirring slowly and left at room temperature for 2 days. The products were dialyzed against double distilled water in a dialysis tube (MWCO 12-14 kDa; Himedia, India) for 72 h followed by lyophilization. The chemical structure of M-chitosan was elucidated through FT-IR (Schimadzu, Model 8400, Japan) and ^{1}H NMR (Jeol AL300 FT-NMR) spectroscopy. FT-IR spectroscopy was carried out using the KBr disk method after adsorption of a smaller amount of substance on KBr and recorded over the range of 4000–400 cm^{-1}. ^{1}H NMR spectroscopy was carried out in the pulsed FT mode at a 300 MHz resonance frequency for protons after dissolving samples in deuterated DMSO.

2.4. Preparation of mannose-conjugated chitosan nanoparticles

RIF loaded M-chitosan nanoparticles were prepared according to the procedure first reported by Calvo, Remunan-Lopez, Vila-Jato, and Alonso (1997) with suitable modifications based on the ionotropic gelation of M-chitosan with TPP anions. Briefly, M-chitosan was dissolved in (2.0 mg/mL) aqueous acetic acid (pH 4.0) solution and TPP was dissolved in purified water at the concentration of 1.2 mg/mL. RIF (10.0%) was added to the TPP solution (RIF dissolved previously in DMSO and diluted suitably with Phosphate buffer; pH 7.4) and stirred for 5 min using magnetic stirrer. Finally, 1.5 mL of drug containing TPP solution was added to 4 mL of the M-chitosan solution through a syringe needle under magnetic stirring at room temperature thereby leading to formation of drug loaded mCNPs at room temperature. The nanoparticles prepared were then sonicated with an ultrasonic power of 100 W and a frequency of 30 kHz for 5 to 20 min. The milky suspension was filtered through a 0.45-μm filter to remove insoluble aggregate residues and then centrifuged at 12,000 rpm at 4 °C for 30 min. The supernatant was discarded and sediment was poured into dialysis bag and dialyzed three times with phosphate buffer saline (pH 7.4) under strict sink conditions for 10 min to remove free drug from the formulation, which was then estimated spectrophotometrically at 333 nm to determine indirectly the amount of drug loaded within the formulation. The dialyzed formulation was lyophilized using sucrose as cryoprotector and used for further characterization. The nonconjugated chitosan nanoparticles (CNPs) were prepared by the same method.

2.5. Characterizations of prepared nanoparticles

Particle size, size distribution and zeta potential of the prepared nanoparticles were determined by light scattering particle sizer (Beckman Coulter, Delsa^{TM} Nano, USA). The particle size distribution was reported as polydispersity index (PDI). Drug entrapment efficiency (EE) of nanoparticles was determined by the method proposed by Vandervoort and Ludwig (2004) and calculated using the following equation:

$$\text{Entrapment efficiency}(\%) = \frac{\text{amount of drug used} - \text{amount of unbound drug}}{\text{amount of drug in the formulation}} \times 100$$

The drug loading (DL) of the RIF in the nanoparticles was determined by assaying both the supernatant after centrifugation and hydrolyzing the known amount of nanoparticles in suitable solvent and measuring the absorbance by UV-visible spectrophotometer at 333 nm. DL and yield were determined using following equations.

$$\text{Drug loading}(\%) = \frac{\text{amount of drug used} - \text{amount of unbound drug}}{\text{amount of nanoparticle recovered}} \times 100$$

$$\text{Nanoparticle yield}(\%) = \frac{\text{amount of recovered nanoparticle}}{\text{total amount of polymer and drug added}} \times 100$$

Selected batches of nanoparticles were subjected to scanning electron microscopy (SEM, QUANTA 200 FEI, Netherlands) and

atomic force microscopy (AFM, NSE Nanoscope-E) for their morphology (shape and size). AFM was operated in contact mode.

2.6. In vitro drug release study

In vitro release study was performed in two media of physiological pH 7.4 and endosomal pH 4.5, using equilibrium dialysis technique. Briefly, 2 mL of nanoparticles dispersion, free from any unentrapped drug, was placed in a dialysis bag (MWCO 12–14 kDa; Himedia, India) and sealed at both the ends. The nanoparticles loaded dialysis bag was then suspended into a beaker containing 100 mL PBS of pH 7.4 or 4.5 containing 0.1 mg/ml L-ascorbic acid, which was added as an antioxidant to prevent oxidative degradation of RIF at a rotation speed of 50 rpm (Guellec, Gaudet, Lamanetre, & Breteau, 1997). Temperature was maintained at $37 \pm 2\,^{\circ}C$ throughout the study. At various time points, aliquot of samples were withdrawn and replaced with the same volume of fresh PBS. The drug content was then determined spectrophotometrically at 333 nm.

2.7. In vivo studies

In vivo study was performed by the methods reported previously (Gulyaev et al., 1999; Reddy & Murthy, 2004). For in vivo studies 60 male albino rats were divided into four groups of 15 rats each. They were fasted overnight with water ad libitum before administration of dose. An aqueous solution of RIF was injected into the tail vein to the animals of first group. Second and third groups received drug-loaded CNPs and mCNPs, respectively, whereas the rats of the fourth group were kept as a control. 500 μL of phosphate buffer saline (PBS; pH 7.4) was used as vehicle and dose level 12 mg/kg body weight of animal was kept constant in each case. Following the drug administration, animals from each group were bled at 30 min, 1, 2, 3, 6, 8, 12 and 24 h through the retro-orbital plexus, blood was collected and serum was separated and analyzed for the drug. In addition, at above mentioned time points, two animals of each group were sacrificed and organs (spleen and liver) were excised, isolated, dried using tissue paper and weighed. Organs and serum were stored at $-80\,^{\circ}C$ until assayed. The experiment was repeated for reproducibility with a further 60 animals and the results were collated. The studies were carried out according to the guidelines of the Council for the Purpose of Control and Supervision of Experiments on Animals, Ministry of Social Justice and Empowerment, Government of India, and also in agreement with the guidelines of the Institutional Animal Ethical Committee of the Banaras Hindu University, Varanasi (U.P.) India.

2.8. Pharmacokinetic study in serum

Collected blood samples were centrifuged at 2000 rpm for 10 min and the serum was harvested. Collected serum was filtered through 0.45 μm-membrane filter (Himedia, India). To 200 μL of serum, 100 μL of acetonitrile was added and the mixture was centrifuged at 2000 rpm for 15 min to remove the proteins. Supernatant was filtered through a 0.45 μm filter and collected into a HPLC vials (Himedia, India). Drug estimation in supernatants was done using a reported HPLC method (Karki, Subramanya, & Udupa, 2009). Calibration curve was obtained by analyzing pooled blank serum spiked with known amounts of drug. The HPLC system (Cecil CE4201 Cambridge, UK), equipped with C-18 column (Phonomenex, 250 × 4.60 mm, Particle size 5 μm) and UV visible detector was used for the estimation of drug. Mobile phase consisted of aqueous acetonitrile (pH 2.27 adjusted with orthophosphoric acid) in (v/v) ratio of 2:3. The mobile phase was filtered through 0.45 μm membrane filter (Himedia, India) and degassed before analysis. Elution was performed at ambient temperature with a flow-rate of 1 mL/min for 10 min.

Various pharmacokinetic parameters were determined using WIN-NON-LIN pharmacokinetic software using serum drug concentration data. Maximum plasma concentration (C_{max}), time taken to reach maximum concentration, (T_{max}) and mean resident time (MRT) were calculated. The area under plasma concentration–time curve $[AUC]_{0-24}$ was determined by the trapezoidal method. The terminal $[AUC]_{24-\infty}$ was obtained by dividing the last measurable plasma concentration by the elimination rate constant which is obtained by regression analysis. The sum of $[AUC]_{0-24}$ and $[AUC]_{24-\infty}$ gave the total $[AUC]_{0-\infty}$ and area under moment curve (AUMC)/area under curve (AUC) gave the mean residence time (MRT) of drug.

2.9. Biodistribution study

Stored organs were recovered from deep freezer and kept outside for some time to come at ambient temperature. Each tissue was then weighed and cut into small pieces. One gram of each organ was homogenized with 2 mL PBS (pH 7.4). In the case of organs weighing less than 1 g, the whole organ was used. 150 mL of tissue homogenate was deproteinized with an equal volume of 10% (v/v) trichloroacetic acid in water, vortexed for 5 min and cold centrifuged (5000 rpm/5 min). Supernatant was filtered through a 0.45 μm membrane filter, analyzed by HPLC and compared with calibration curve for drug content. Calibration curve was obtained by analyzing pooled blank organ homogenates spiked with known drug amount.

2.10. Ex vivo cellular uptake studies

2.10.1. Harvesting and viability testing of macrophages

Activated macrophages were harvested from the peritoneal cavity of male rats, deeply anesthetized with ketamine (50 mg/kg of body weight, intraperitoneal). The harvested cell suspension was cold centrifuged at 1500 rpm for 10 min and the obtained cell pellet was resuspended in HEPES (4-(2-hydroxyethyl)-1-piperazineethanesulfonic acid) buffer. The dye exclusion test was used to determine the number of viable cells present in a cell suspension (Torres-Lugo, Garcia, Record, & Peppas, 2002). It is based on the principle that live cells possess intact cell membranes that exclude certain dyes, such as trypan blue, eosin, or propidium, whereas dead cells do not. In our study, 10 μL of cell suspension was simply mixed with equal amount of 0.4% trypan blue dye. Mixture was allowed to incubate for 3 min at room temperature and then within 3–5 min of mixing, visually counted with Neubauer hemocytometer to determine whether cells take up or exclude the dye. Viable cells excluded the dye and showed clear cytoplasm whereas nonviable cells showed blue cytoplasm.

2.10.2. Cell uptake study

For ex vivo cellular uptake experiments, cells were washed twice with 1 mL (pH 7.4) Hank's balanced salt solution (HBSS). Cells with seeding density of 1×10^5 cells/mL were plated on 12-well Falcon culture plates (Tarsons products Ltd. India) in RPMI 1640 media supplemented with 10% heat-inactivated fetal calf serum (FCS) (Himedia, India) and 1% antibiotics (Liang, Shi, Deshpande, Malanga, & Rojanasakul, 1996). After 6 h of incubation at controlled conditions ($37\,^{\circ}C$, 5% CO_2 and 95% O_2), nonadherent macrophages were washed off with culture medium and cells were treated with FITC labeled CNPs and mCNPs at the same dose level and cultured under the same conditions (Tiwari, Chaturvedi, Tripathi, & Mishra, 2011). For quantitative drug estimation, study was carried out for 24 h. At the end of 24 h cells were recovered from the culture plate and subjected to repetitive washing and centrifugation

Table 1
Degrees of substitution with different raw material ratios.

Sample	C (%)	H (%)	N (%)	O (%)	DS (%)
Chitosan	44.72	6.83	8.69	39.75	–
M-chitosan	44.59	6.90	7.35	41.15	17.67

(5000 rpm/3 min) with ice-cold phosphate buffer saline (PBS) three times. Supernatants were pooled together to quantify the surface bound drug whereas cell pellets were used for the intracellular drug estimation. For the intracellular drug estimation, cell pellets was homogenized in distilled deionized water (100 μL), sonicated on ice (3 cycles/60 s) and estimated by HPLC.

Qualitative cellular uptake study was performed to visualize the interaction of nanoparticles with macrophage cells. For this, FITC labeled CNPs and mCNPs (2 mg/well) were added to the culture plates containing the previously harvested macrophages. They were incubated for 2 h at 37 °C and 5% CO_2. Peritoneal macrophages (PMs) were finally fixed with an aqueous solution of 8% (v/v) formaldehyde and visualized under confocal microscope (LSM, 510 META, Zeiss, Germany). CLSM (Confocal laser scanning microscopy) scanning was performed using 20× Plan Aprochromat objective, having a numerical aperture of 0.8. Images were taken at an excitation wavelength of 488 nm and band pass of 505–550 nm. Maximum power 20% was used.

3. Results and discussion

3.1. Physicochemical characterization of M-chitosan

Mannose-conjugation of chitosan was undertaken with a view to increase their uptake by the macrophage of reticuloendothelial system (RES) through receptor-mediated endocytosis. In our knowledge, this is the first study reporting the successful delivery of mCNPs, in terms of internalization to macrophages via intravenous administration, since internalization is a crucial factor affecting the efficiency of delivery systems. Therefore, it was expected to have information not only about the potential of chitosan nanoparticles for increasing concentration of drug to the site (macrophages of RES) but also for their selective and preferential localization in macrophages for effective treatment of VL.

M-chitosan was prepared by reductive amination of chitosan with D-mannose in the presence of reductive aminating agent, sodium triacetoxyborohydride [$NaBH(OAc)_3$]. This reagent is mild and exhibits remarkable selectivity as a reducing agent. It reduces aldehydes selectively over ketones (Abdel-Magid, Carson, Harris, Maryanoff, & Shah, 1996). The degree of substitution (DS) of mannose was determined by elemental analysis. Elemental compositions of chitosan and M-chitosan were recorded on an Exeter CE 440 elemental analyzer (UK). The percentages of carbon, hydrogen and nitrogen were estimated. The DS of mannose that was determined from C, H, and N analyses was found to be 17.67% (Table 1).

FT-IR spectrum of mannose, chitosan and M-chitosan was compared in Fig. 1. A band at 3423.76 cm^{-1} indicated the presence of $-NH_2$ and $-OH$ group stretching vibration in chitosan. A strong N—H bending at 1595.18 cm^{-1} revealed the presence of primary amine groups in chitosan (Fig. 1A).

Mannose-conjugation took place by ring opening of mannose followed by reaction of its aldehyde group with free amino groups of chitosan (Gribble & Ferguson, 1975). This leads to the formation of Schiff's base (R—CH=N—R bond) which was confirmed by the presence of N—H bending of secondary amines at 1558.54 cm^{-1} and C=N stretch at 1410.01 cm^{-1}. Also, the shifting of peak from 3304.17 to 3383.26 cm^{-1} and its broadening supported the aforesaid statement (Fig. 1B).

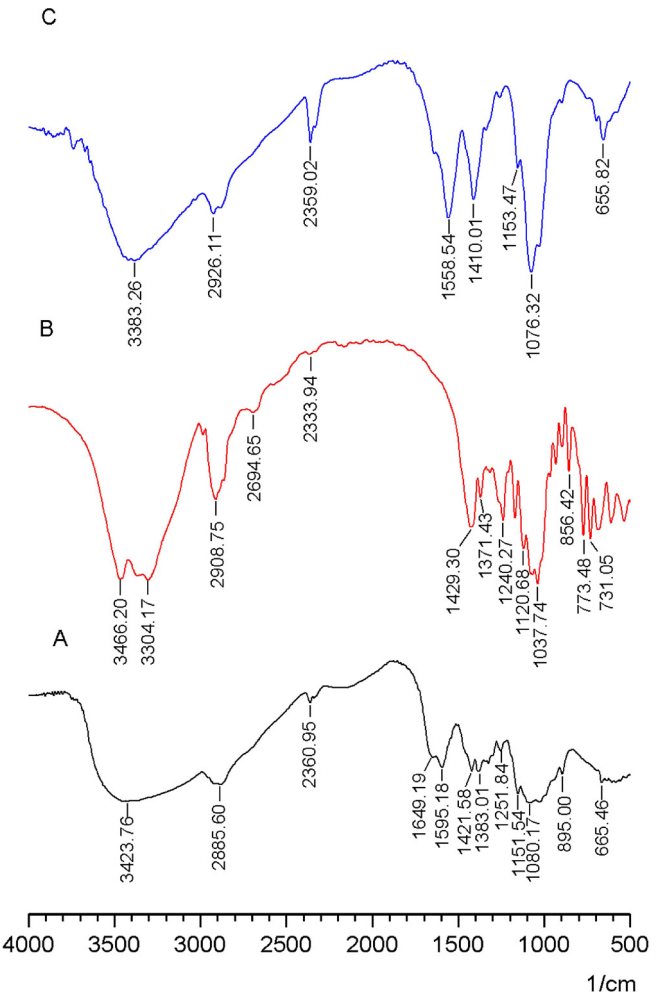

Fig. 1. FT-IR spectra of: (A) chitosan, (B) mannose, and (C) lyophilized M-chitosan (Data were collected over 50 scans at 4° resolution).

^1H NMR study was performed for chitosan and M-chitosan. The peaks and shifts of ^1H NMR spectrum of M-chitosan as compared with that of chitosan give strong proof of mannosylation. Chitosan showed peaks of alkane at 1.22 ppm, peaks of alkyl amine at 1.89 ppm, peaks of aldehyde group at 3.39 ppm. On mannosylation, a very strong peak at 1.89 ppm was observed which could be contributed to the proton of $-CH_2-$ which was the bridge for linking mannose to chitosan. A strong peak at 2.5 ppm in case of chitosan was observed which is due to proton present at chitosan ring, to which $-NH_2$ group is attached. After mannosylation, this proton will be sterically hindered by mannose moiety and therefore a weak peak at 2.49 is observed in case of M-chitosan. Also, a strong peak at 1.89 ppm in case of M-chitosan compared to chitosan given a strong proof of mannosylation. The strong peak is due to protons contributed by mannose group in M-chitosan which are absent in chitosan. Further, elemental compositions of chitosan and M-chitosan were recorded on an Exeter CE 440 elemental analyzer (UK). The percentages of carbon, hydrogen, nitrogen and oxygen were estimated. The degree of substitution (DS) of mannose that was determined from C, H, N and O analyses was 17.67% (Table 1). These findings provided us an obvious evidence of successful conjugation of mannose with chitosan.

Table 2
Characterization of drug loaded CNPs and mCNPs.[a]

Formulation Code	Particle Size (nm)	Polydispersity index	Zeta Potential (mV)	Entrapment efficiency (%)	Yield (%)
CNPs	181.7 ± 3.7	0.137 ± 0.24	39.6 ± 2.3	43.7 ± 2.7	84 ± 2.6
mCNPs	215.2 ± 2.4*	0.109 ± 0.18	26.2 ± 1.7*	39.1 ± 6.3*	79 ± 5.4**

[a] All data are shown as mean ± S.D.; $n = 6$. * $p < 0.05$. ** $p < 0.5$

3.2. Characterization of prepared nanoparticles

mCNPs and CNPs were prepared by ionic gelation method via Schiff's base formation with TPP. The free amino groups of M-chitosan and chitosan took part into ionic cross linking and lead to the formation of mCNPs and CNPs, respectively. The morphology of prepared nanoparticles was analyzed under SEM (Fig. 2) and AFM (Supplementary data). The SEM image of M-chitosan revealed that mannose conjugation modified the surface morphology of chitosan significantly. Chitosan showed spherulites like structure (Fig. 2A) while covalent coupling between mannose and chitosan have resulted into formation of cohesive strands of M-chitosan (Fig. 2B). SEM micrographs also revealed the smooth surface and spherical shape of nanoparticles (Fig. 2C and D). The average particle size of mCNPs was found to be 215 nm as compared with the particle size of nonconjugated CNPs, which was 181 nm (Table 2). This could be due to anchoring of mannose molecules to the chitosan polymers. The ability of nanoparticles to alter the pharmacokinetics and biodistribution of drugs has important in vivo therapeutic applications (Davis, 1997). Thus, the size and surface characteristics of nanoparticles are of prime importance. Nanoparticles of particle size >100 nm are easily captured by Kupffer cells or other phagocytic cells of RES and restrict their biodistribution to other non-target organs (Wisse & Leeuw, 1984). A very low polydispersity index was obtained for both formulations, indicating a narrow size distribution of the nanoparticles and consequently a homogeneous distribution. The average zeta potential of mCNPs (26.2 mV) was found to be lower than that of CNPs (39.6 mV) ($p < 0.05$). The decrease in zeta potential of mCNPs was due to the fact that the conjugation of mannose to chitosan resulted in the reduction of the primary amino groups of chitosan as NH_2 of chitosan couples to CHO groups of mannose. The low surface charge of the mCNPs is fit for use in vivo due to the low reaction with components of the in vivo environment (Zhou et al., 2007). Further, the photomicrographs of AFM established their nanometric size and that the nanoparticles are well dispersed as individual particles.

3.3. In vitro drug release study

In vitro RIF release data are presented in Fig. 3. Release study was performed at two different pH values; physiological pH 7.4 and endosomal pH 4.5 by buffer change method. The results have shown that 11.42% and 9.37% RIF were released within first 2 h (at physiological pH 7.4) from CNPs and mCNPs, respectively while more than 90% drug was released from both the formulations in next 3 h (at endosomal pH 4.5). An initial burst release of RIF from both the formulations could be due to adsorbed drug on the surface or present just beneath the surface of nanoparticles.

Both unconjugated and mannose-conjugated nanoparticles release more than 90% of drug at endosomal pH of 4.5. This faster release at endosomal pH may be due to insoluble nature of chitosan and RIF at physiological pH (pH 7.4) and solubility of both at endosomal pH (pH 4.5). Therefore, the results of release study were found according to our goal as majority of drug would release inside the cell following endocytosis of the carrier system. Besides, the insoluble nature of chitosan and RIF at basic pH (physiological

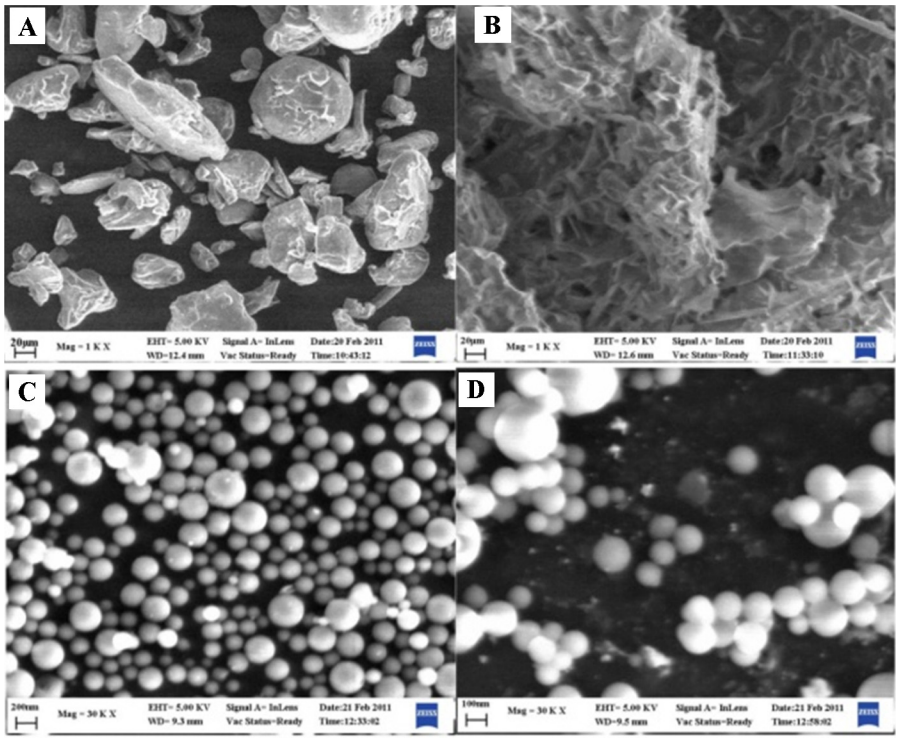

Fig. 2. SEM micrographs of (A) chitosan, (B) M-chitosan, and RIF loaded (C) CNPs, (D) mCNPs (1 mg samples were mounted on an aluminum support, sputter coated and analyzed at an operation voltages of 5.00 kV.

Table 3
Comparison of pharmacokinetic parameters following intravenous administration of free drug solution, CNPs and mCNPs in to albino rats at the dose of 12 mg RIF/kg.[a]

Dosage form	C_{max} (μg/mL)	$T_{1/2}$ (h)	$AUC_{0-24\,h}$ (μg h/mL)	$AUC_{0-\infty}$ (μg h/mL)	MRT (h)
RIF solution	279.00 ± 17.71	1.69 ± 0.63	384.75 ± 27.12	394.48 ± 31.52	1.82 ± 0.2
CNPs	25.31 ± 2.46*	17.47 ± 1.52*	290.95 ± 3.81*	535.46 ± 23.10*	28.13 ± 3.3*
mCNPs	5.40 ± 1.64*,**	40.42 ± 2.81*,**	177.47 ± 21.90*,**	533.26 ± 22.01*	58.48 ± 9.1*,**

[a] All data are shown as mean ± S.D.; $n = 6$. *$p < 0.05$ vs. RIF solution. **$p < 0.05$ vs. CNPs.

Table 4
Organ distribution of RIF following intravenous administration of various formulations given at the dose of 12 mg/kg body weight of rat.[a]

Notation	Organ	Percentage (%) of dose recovered after						
		30 min	1 h	2 h	3 h	6 h	12 h	24 h
Free	Liver	18.6 ± 1.2	25.2 ± 0.7	19.1 ± 1.5	12.8 ± 1.6	6.91 ± 1.3	1.7 ± 0.7	ND[b]
RIF	Spleen	5.3 ± 1.4	4.7 ± 1.1	4.1 ± 1.2	3.1 ± 1.2	1.1 ± 0.2	ND[b]	ND[b]
CNPs	Liver	30.8 ± 1.3	38.1 ± 1.1	50.2 ± 0.3	47.1 ± 1.6	43.3 ± 2.1	37.8 ± 3.2	32.9 ± 1.7
	Spleen	4.3 ± 1.8	6.9 ± 2.8	8.7 ± 0.4	7.5 ± 1.1	6.1 ± 1.2	4.5 ± 0.8	3.9 ± 0.7
mCNPs	Liver	37.8 ± 1.7*	52.9 ± 2.6*	71.2 ± 1.8*	63.4 ± 0.9*	57.5 ± 1.3*	53.1 ± 3.4*	50.6 ± 2.2*
	Spleen	12.6 ± 1.8*	16.7 ± 2.5*	19.4 ± 1. 4*	16.8 ± 1.1*	14.2 ± 1.5*	12.8 ± 0.2*	11.1 ± 1.2*

[a] All the values are mean ± S.D. [b]ND: not detected, $n = 6$ animals at each time duration. *$p < 0.05$ vs. CNPs and Free RIF.

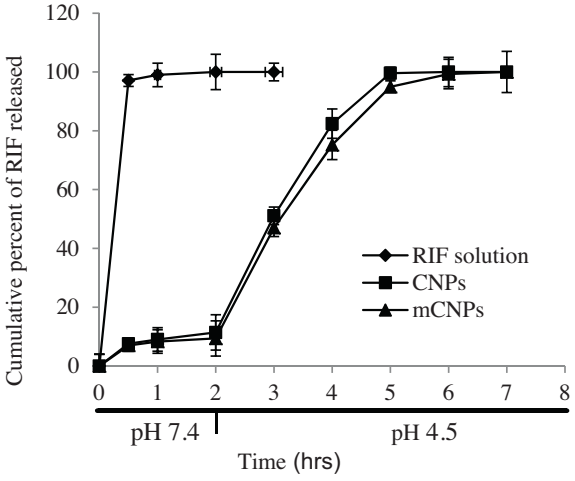

Fig. 3. In vitro release profile of RIF from the prepared nanoparticles (bars represent ± standard deviation; $n = 3$). Release study was performed at two different pH values; at physiological pH 7.4 for 2 h and for next 6 h at endosomal pH 4.5 by buffer change method.

pH) would minimize the chances of drug release into the general circulation before macrophage engulfment and hence potentiates the efficient delivery to the target cells.

3.4. In vivo pharmacokinetic and biodistribution studies

The results of both the sets of in vivo studies involving 60 animals in each set were merged and mean values were taken for analysis. The in vivo studies clearly revealed that the pharmacokinetics and biodistribution of RIF were significantly altered when delivered through mannose-conjugated nanoparticles (mCNPs). Pharmacokinetic data in Table 3 clearly indicate that the free RIF solution rapidly cleared off from the blood circulation and was detected only till the 12th hour following single intravenous administration.

In contrast, blood level in the case of CNPs and mCNPs remained for a longer period, though; the blood level of mCNPs was lower than that of CNPs at each time point. This may be due to the relatively rapid uptake of mCNPs by macrophage-rich organs (organs of RES; liver, spleen etc.) in comparison to CNPs. Also, the data shown in Table 3 clearly indicate that mannose conjugation resulted into significant improvement in the value of MRT (mean residence time) ($p < 0.05$; one-way ANOVA).

The biodistribution studies were performed to investigate the in vivo target specificity of mCNPs formulations. The concentration of RIF in different organs was estimated by HPLC (Table 4).

The result indicated a significantly higher accumulation of drug in the macrophage rich organs (liver and spleen) in case of both the nanoparticulate formulations as compared to plain RIF solution. Eventually, mCNPs exhibit significantly higher accumulation of RIF than CNPs ($p < 0.05$; one-way ANOVA) and clearly indicate the superiority over CNPs. The MRT of RIF in these organs delivered through mCNPs after i.v. injection was significantly higher than free drug solution. The estimated amount of drug in liver and spleen revealed that maximum accumulation of the drug in these organs was achieved within 1–2 h following intravenous administration. The accumulation of drug in different macrophage rich organs from mCNPs (71.2% in liver and 19.4% in spleen) and CNPs (50.2% in liver and 8.7% in spleen) was significantly higher ($p \leq 0.05$; one-way ANOVA) as compared to free drug after 2 h (Table 4). The higher accumulation of RIF in spleen and liver, in case of mannose-conjugated nanoparticles, probably occurred owing to the specific uptake of mCNPs by macrophages. It has been demonstrated elsewhere (Chono, Tanino, Seki, & Morimoto, 2007; Ghosh, Das, & Bacchhawat, 1982) that mannose-conjugated carrier systems up-regulates the activity of mannose receptors over surface of macrophages of RES. Thus, a surface mannose modification of chitosan is thought to be the rationale behind preferential uptake by macrophages. As a result, there was much lower blood level of RIF and no sharp peaks were observed. Therefore, results of the study indicate targeting prospective, spatial delivery, enhanced bioavailability and increased retention potential of mCNPs in the macrophage rich organs.

3.5. Ex vivo cellular uptake studies

Since the internalization of carrier is important and crucial factor for the success of targeted delivery systems (Wijagkanalan et al., 2008), ex vivo drug uptake studies of the developed formulations was performed in cultured macrophages. A significant increase in cellular drug uptake was observed when mCNPs were used, which was 16.2 and 2.3 times higher than that of free drug ($p \leq 0.05$) and unconjugated CNPs ($p \leq 0.05$) at 24 h, respectively (Supplementary data). Particulate carriers are opsonic materials which has great tendency to get engulfed by macrophages of reticuloendothelial system (RES), whereas drug solution will have a tendency of

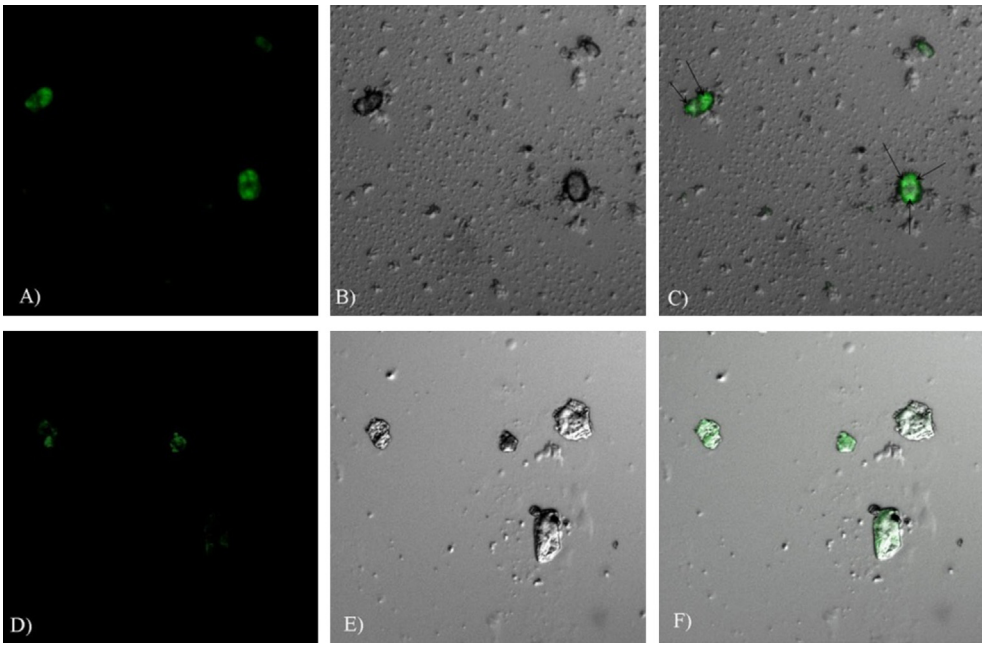

Fig. 4. Confocal laser scanning microscopic images showing endocytosis of mCNPs (A–C) and CNPs (D–F) in macrophages, isolated from rat peritoneal fluid. (A and D) Fluorescent micrograph, (B and E) DIC image, (C and F) merge of fluorescent and DIC image. Scanning was performed using 20× Plan Aprochromat objective, having a numerical aperture of 0.8. Images were taken at an excitation wavelength of 488 nm with band pass of 505–550 nm. Maximum power 20% was used in the study. In Figure C black arrow indicate the macrophage cells containing FITC-labeled mCNPs.

undergoing distribution rather than being internalized specifically by the cells. Mannose-conjugation of the carrier systems further enhanced the uptake via mannose receptor-mediated mechanism in macrophages. To verify the uptake mechanism of mCNPs via the mannose receptor mediated process in macrophages, isolated macrophages were incubated with 0.05 M mannose (a corresponding sugar inhibitor) in a parallel experiment and result reported a drastic reduction of cellular internalization of mCNPs (Supplementary data). It provided us the evidence that uptake of mannosylated carriers occurred via mannose receptor mediated endocytosis (Jiang et al., 2008).

The extensive internalization of mCNPs was demonstrated by the in vitro CLSM micrographs (Fig. 4) corresponding to the in vitro uptake study. The CLSM micrographs suggested that within 2 h of the administration of the FITC labeled mCNPs, strong intracellular fluorescence was observed in the cytosol of macrophages which was indicative of the enhanced uptake of mCNPs via a mannose receptor mediated mechanism in macrophages.

Translating this prompt internalization and distribution behavior of the formulation in terms of its therapeutic effectiveness, the mannose-conjugated chitosan carrier system could be proposed to be more interesting since more amount of drug could be internalized within the RES macrophages too (similar to peritoneal macrophages), which constitute the desired site of action for anti-leishmanial drugs. Such treatment modality is expected to avoid the chances of resistance, pathogen persistence and recurrent infections. The studies are indicative of a good targeted drug delivery system; however, it would be used further for preclinical evaluation of anti-leishmanial activity and the toxicity.

4. Conclusion

In this study, mCNPs were successfully synthesized and evaluated as a novel drug delivery carrier for macrophage targeting using surface functionalized M-chitosan. FT-IR and ^{1}H NMR datas of the prepared conjugate (M-chitosan) were in agreement to the presumptive pathway of reaction. The strong intracellular fluorescence observed in CLSM studies provide evidence that endocytosis took place effectively inside the macrophages. In vivo biodistribution and pharmacokinetic studies of mCNPs resulted in a significantly higher concentration of RIF in spleen, and liver. Nanoparticles formulated from the M-chitosan provided satisfactory loading efficiency and drug release characteristics. They offered desirable size range for macrophages engulfment and possessed a uniform size distribution. Thus, mCNPs represent efficient, viable, safe, and cheaper novel-targeted delivery system of RIF as an alternative to lipid-based formulations for the treatment of VL. Further, such carriers hold potential to increase the efficacy and reduce the toxicity of macrophages-specific delivery of bioactives and might be effective for other intracellular tissue macrophages-specific deadly diseases such as HIV, tuberculosis. This system could also present putative advantages in the treatment of VL associated with tuberculosis. However, further studies are warranted to investigate the toxicity and biodegradation aspects of mCNPs as different set of cells can differ in their biological response toward the proposed carrier.

Conflict of interest

The authors report no conflicts of interest. The authors alone are responsible for the content and writing of the paper.

Acknowledgements

One of the authors (P. Chaubey) is thankful to University Grant Commission, New Delhi, India for providing financial assistance (SRF) to carry out this research work. The support of Prof. G.V.S. Sastry (Department of Metallurgical Engineering), Prof. S.C. Lakhotia (Department of Zoology), Prof. Y.B. Tripathi (Department of Medicinal Chemistry, Institute of Medical Sciences) of Banaras Hindu University is thankfully acknowledged for providing the facility of SEM, CLSM and ex vivo studies, respectively. I also would like to thank UGC-DAE, CSR, Indore for providing AFM facility.

References

Abdel-Magid, A. F., Carson, K. G., Harris, B. D., Maryanoff, C. A., & Shah, R. D. (1996). Reductive amination of aldehydes and ketones with sodium triacetoxyborohydride studies on direct and indirect reductive amination procedures. *Journal of Organic Chemistry*, *61*, 3849–3862.

Bakker-Woudenberg, I. A. J. M. (1995). Delivery of antimicrobials to infected tissue macrophages. *Advanced Drug Delivery Reviews*, *17*, 5–20.

Busilacchi, A., Gigante, A., Mattioli-Belmonte, M., Manzotti, S., & Muzzarelli, R. A. A. (2013). Chitosan stabilizes platelet growth factors and modulates stem cell differentiation toward tissue regeneration. *Carbohydrate polymers*, *98*, 665–676.

Calvo, P., Remunan-Lopez, C., Vila-Jato, J. L., & Alonso, M. J. (1997). Novel hydrophilic chitosan-polyethylene oxide nanoparticles as protein carriers. *Journal of Applied Polymer Science*, *63*, 125–132.

Chellat, F., Merhi, Y., Moreau, A., & Yahia, L. (2005). Therapeutic potential of nanoparticulate systems for macrophage targeting. *Biomaterials*, *26*, 7260–7275.

Chono, S., Tanino, T., Seki, T., & Morimoto, K. (2007). Uptake characteristics of liposomes by rat alveolar macrophages: Influence of particle size and surface mannose modification. *Journal of Pharmacy and Pharmacology*, *59*, 75–80.

Davis, S. S. (1997). Biomedical applications of nanotechnology-implications for drug targeting and gene therapy. *Trends in Biotechnology*, *15*, 217–224.

Duncan, R. (2003). The dawning era of polymer therapeutics. *Nature Reviews Drug Discovery*, *2*, 347–360.

Ferrari, G., Langen, H., Naito, M., & Pieters, J. (1999). A coat protein on phagosomes involved in the intracellular survival of mycobacteria. *Cell*, *14*, 435–447.

Ghosh, P., Das, P. K., & Bacchhawat, B. K. (1982). Targeting of liposomes towards different cell types of rat liver through the involvement of liposomal surface glycosides. *Archives of Biochemistry and Biophysics*, *213*, 266–270.

Gribble, G. W., & Ferguson, D. C. (1975). Selective reduction of aldehydes with sodium triacetoxyborohydride. *Journal of the Chemical Society, Chemical Communications*, 535–536.

Guellec, C. L., Gaudet, M. L., Lamanetre, S., & Breteau, M. (1997). Stability of rifampicin in plasma: consequences for therapeutic monitoring and pharmacokinetic studies. *Therapeutic Drug Monitoring*, *19*, 669–674.

Gulyaev, A. E., Gelperina, S. E., Skidan, I. N., Antropov, A. S., Kivman, G. Y., & Kreuter, J. (1999). Significant transport of doxorubicin into the brain with polysorbate 80-coated nanoparticles. *Pharmaceutical Research*, *16*, 1564–1569.

Jain, S. K., Gupta, Y., Jain, A., Saxena, A. R., Khare, P., & Jain, A. (2008). Mannosylated gelatin nanoparticles bearing an anti-HIV drug didanosine for site-specific delivery. *Nanomedicine: NBM*, *4*, 41–48.

Jiang, H. L., Kang, M. L., Quan, J. S., Kang, S. G., Akaike, T., Yoo, H. S., et al. (2008). The potential of mannosylated chitosan microspheres to target macrophage mannose receptors in an adjuvant-delivery system for intranasal immunization. *Biomaterials*, *29*, 1931–1939.

Karki, R., Subramanya, G., & Udupa, N. (2009). Formulation and evaluation of coencapsulated rifampicin and isoniazid liposomes using different lipids. *Acta Pharmaceutica Sciencia*, *51*, 177–188.

Liang, W. W., Shi, X., Deshpande, D., Malanga, C. J., & Rojanasakul, Y. (1996). Oligonucleotide targeting to alveolar macrophages by mannose receptor-mediated endocytosis. *Biochimica et Biophysica Acta*, *1279*, 227–234.

Marty, P., & Rosenthal, E. (2002). Treatment of visceral leishmaniasis: a review of current treatment practices. *Expert Opinion on Pharmacotherapy*, *3*, 1101–1108.

Murray, W. H. (2004). Treatment of visceral leishmaniasis in 2004. *The American Journal of Tropical Medicine and Hygiene*, *71*, 787–794.

Muzzarelli, R. A. A. (2010). Chitins and chitosans as immunoadjuvants and non-allergenic drug carriers. *Marine Drugs*, *8*, 292–312.

Neuber, H. (2008). Leishmaniasis. *Journal der Deutschen Dermatologischen Gesellschaft*, *9*, 754–765.

Reddy, L. H., & Murthy, R. S. R. (2004). Pharmacokinetics and biodistribution studies of doxorubicin loaded poly(butyl cyanoacrylate) nanoparticles synthesized by two different techniques. *Biomedical Papers*, *148*, 161–166.

Rinaudo, M. (2006). Chitin and chitosan: Properties and applications. *Progress in Polymer Science*, *31*, 603–632.

Sakuma, H., & Ohshima, T. K. (1990). Binding constants of metal cations to and Hamaker constant for poly (NN-lysine diylterephthaloyl) microcapsules. *Journal of Colloid and Interface Science*, *135*, 455–460.

Seferian, P. G., & Martinez, M. L. (2001). Immune stimulating activity of two new chitosan containing adjuvant formulation. *Vaccine*, *19*, 661–668.

Tiwari, S., Chaturvedi, A. P., Tripathi, Y. B., & Mishra, B. (2011). Macrophage specific targeting of isoniazid through mannosylated gelatin microspheres. *AAPS PharmSciTech*, *12*, 900–908.

Torres-Lugo, M., Garcia, M., Record, R., & Peppas, N. A. (2002). Physicochemical behavior and cytotoxic effects of p(methacrylic acid-g-ethylene glycol) nanospheres for oral delivery of proteins. *Journal of Controlled Release*, *80*, 197–205.

Vandervoort, J., & Ludwig, A. (2004). Preparation and evaluation of drug-loaded gelatin nanoparticles for topical ophthalmic use. *European Journal of Pharmaceutics and Biopharmaceutics*, *57*, 251–261.

Wadhwa, M. S., & Rice, K. G. (2003). Receptor mediated glycotargeting. *Journal of Drug Targeting*, *11*, 255–268.

Wijagkanalan, W., Kawakami, S., Takenaga, M., Igarashi, R., Yamashita, F., & Hashida, M. (2008). Efficient targeting to alveolar macrophages by intratracheal administration of mannosylated liposomes in rats. *Journal of Controlled Release*, *125*, 121–130.

Wisse, E., & Leeuw, A. M. (1984). Structural elements determining transport and exchange process in the liver. In S. S. Davis, L. Illum, J. G. McVie, & E. Tomlinson (Eds.), *Microspheres and drug therapy, pharmaceutical, immunological and medical aspects* (pp. 1–23). Amsterdam: Elsevier.

Yalpani, M., & Laurance, D. H. (1984). Some chemical and analytical aspects of polysaccharide modifications 3. Formation of branch-chain, soluble chitosan derivatives. *Macromolecules*, *17*, 272–281.

Yeeprae, W., Kawakami, S., Yamashita, F., & Hashida, M. (2006). Effect of mannose density on mannose receptor-mediated cellular uptake of mannosylated o/w emulsions by macrophages. *Journal of Controlled Release*, *114*, 193–201.

Zhou, X., Liu, B., Yu, X., Zha, X., Zhang, X., Chen, Y., et al. (2007). Controlled release of PEI/DNA complexes from mannose-bearing chitosan microspheres as a potent delivery system to enhance immune response to HBV DNA vaccine. *Journal of Controlled Release*, *121*, 200–207.